Cancer Research

TLR Adaptor Protein MYD88 Mediates Sensitivity to HDAC Inhibitors via a Cytokine-Dependent Mechanism

Maria New[1], Semira Sheikh[1], Mina Bekheet[1], Heidi Olzscha[1], Marie-Laetitia Thezenas[2], Matthew A. Care[3,4], Susan Fotheringham[1], Reuben M. Tooze[3], Benedikt Kessler[2], and Nicholas B. La Thangue[1]

Abstract

Histone deacetylase (HDAC) inhibitors have proven useful therapeutic agents for certain hematologic cancers. However, HDAC inhibition causes diverse cellular outcomes, and identification of cancer-relevant pathways within these outcomes remains unresolved. In this study, we utilized an unbiased loss-of-function screen and identified the Toll-like receptor (TLR) adaptor protein MYD88 as a key regulator of the antiproliferative effects of HDAC inhibition. High expression of MYD88 exhibited increased sensitivity to HDAC inhibitors; conversely, low expression coincided with reduced sensitivity. MYD88-dependent TLR signaling controlled cytokine levels, which then acted via an extracellular mechanism to maintain cell proliferation and sensitize cells to HDAC inhibition. MYD88 activity was directly regulated through lysine acetylation and was deacetylated by HDAC6. MYD88 was a component of a wider acetylation signature in the ABC subgroup of diffuse large B-cell lymphoma, and one of the most frequent mutations in MYD88, L265P, conferred increased cell sensitivity to HDAC inhibitors. Our study defines acetylation of MYD88, which, by regulating TLR-dependent signaling to cytokine genes, influences the antiproliferative effects of HDAC inhibitors. Our results provide a possible explanation for the sensitivity of malignancies of hematologic origin to HDAC inhibitor–based therapy. *Cancer Res; 76(23); 6975–87. ©2016 AACR.*

Introduction

Abnormal epigenetic control is a common feature of tumorigenesis, and aberrant lysine acetylation is believed to take on an important role in driving the malignant phenotype (1). Lysine acetylation is regulated by two groups of enzymes, with histone acetyl-transferases (HAT) mediating the acetylation event, and histone deacetylases (HDAC) providing the deacetylation event (2). This type of relationship, often referred to as "writer, reader, and eraser", plays an instrumental role in epigenetic control, where lysine acetylation provides a key regulatory event (1). Furthermore, HAT and HDAC, and bromodomain reader proteins, are families with multiple members, reflecting the diverse biological roles that these enzymes and reader proteins undertake (2, 3). Lysine acetylation occurs on proteins with diverse biological functions, for example, many proteins involved with metabolism and cell signaling (4, 5), and thus acetylation cannot be viewed as a modification that is restricted to the nucleus and epigenetic control.

There is increasing recognition that lysine acetylation is deregulated in cancer, either through mutation in HAT genes or conversely deregulation of HDAC activity (6).

HDACs have been increasingly recognized as a relevant therapeutic target in neoplastic disease (7, 8). Small-molecule inhibition of HDAC activity has antiproliferative effects on cancer cells, including cell-cycle arrest and apoptosis (9), and consequently there has been considerable interest in progressing HDAC inhibitors into clinical studies (2, 10, 11). Some HDAC inhibitors have been approved for clinical use, for example SAHA/vorinostat for treating cutaneous T-cell lymphoma (CTCL), and panobinostat for multiple myeloma (10, 12, 13). It remains unclear how HDAC inhibitors should be optimally deployed for clinical benefit, reflecting the pleiotropic and diverse cellular mechanisms that are controlled by acetylation, and lack of knowledge about how these mechanisms are influenced by HDAC inhibitors and in malignant disease.

To address this question, we have taken an unbiased loss-of-function screening approach to identify pathways that influence the effect of HDAC inhibitors on cancer cells. Here, we report that the Toll-like receptor (TLR) adaptor protein MYD88 regulates cell sensitivity to HDAC inhibitor treatment. MYD88 (myeloid differentiation primary response gene 88) augments TLR-dependent signaling, thereby affecting the level

[1]Department of Oncology, University of Oxford, Oxford, United Kingdom. [2]Target Discovery Institute, Nuffield Department of Medicine, University of Oxford, Oxford, United Kingdom. [3]Section of Experimental Haematology, Leeds Institute of Cancer and Pathology, University of Leeds, Leeds, United Kingdom. [4]Bioinformatics Group, School of Molecular and Cellular Biology, University of Leeds, Leeds, United Kingdom.

Note: Supplementary data for this article are available at Cancer Research Online (http://cancerres.aacrjournals.org/).

M. New, S. Sheikh, and M. Bekheet contributed equally to this article.

Corresponding Author: Nicholas B. La Thangue, University of Oxford, Old Road Campus Research Building, Roosevelt Drive, Oxford OX3 7DQ, United Kingdom. Phone: 44-18-6561-7090; Fax: 44-18-6561-7092; E-mail: nick.lathangue@oncology.ox.ac.uk

doi: 10.1158/0008-5472.CAN-16-0504

of extracellular cytokines, which act in part through an autocrine mechanism to sensitize cells to HDAC inhibition. Notably, MYD88 is a direct target for lysine acetylation, and its deacetylation is mediated by HDAC6. Significantly, hypoacetylation of MYD88 causes enhanced IL6 levels, which sensitizes cells to HDAC inhibition. MYD88 is expressed at high levels and its gene is a target for somatic mutation in hematologic malignancy (14, 15), and cells expressing the most frequently observed mutation, L265P, exhibit enhanced sensitivity to HDAC inhibitors. Furthermore, MYD88 is a component of a wider acetylation signature in the ABC subgroup of diffuse large B-cell lymphoma (DLBCL). Thus, the role of MYD88 in TLR-dependent signaling defines a novel mechanism that sensitizes tumor cells to HDAC inhibitors. Our results bear on the apparent sensitivity of malignancies of hematologic origin to HDAC inhibitor–based therapy.

Materials and Methods

Cell lines

U2OS cells were from ATCC. Cells were regularly tested with a Lonza mycoplasma kit. Regular immunofluorescence microscopy with nuclear staining confirmed a negative mycoplasma result (last negative test November 2015). Cells were passaged twice a week and used until 16 passages. The inducible U2OS-stable cell lines were thawed before each experiment. RIVA and HBL-1 cells were from Prof. Alison Banham (May 2013; Haemato-oncology, Nuffield Division of Clinical Laboratory Sciences, John Radcliffe Hospital, Oxford, United Kingdom) at passage 8. MYD88 L265P mutation status was confirmed in both cell lines (December 2013) by DNA sequencing. Mycoplasma testing was carried out as above (last negative test May 2016). U2OS cells were maintained in DMEM supplemented with 10% FCS and 1% penicillin/streptomycin (Invitrogen). RIVA and HBL-1 cells were maintained in RPMI supplemented with the same. The inducible FLAG-MYD88 cells were created in parental U2OS cells using the Clontech Tet-On gene expression system (Clontech). Ectopic FLAG-protein expression was induced by doxycycline according to manufacturer's instructions. HDAC6 shRNA knockdown U2OS cell lines were created in U2OS cells using HDAC6 or control shRNA lentiviral particles (Santa Cruz Biotechnology), and stable clones were selected for puromycin resistance as per the manufacturer's protocol.

Plasmids, transfection, and screen

Cells were transfected using GeneJuice (Merck) and harvested 24 to 72 hours after transfection. U2OS cells were transfected with siRNAs against HDAC6 (Dharmacon, M-00349900), MYD88 (Smart-Pool Dharmacon), and nontargeting control NT2 (Dharmacon) using oligofectamine (Invitrogen) to a final concentration of 50 nmol/L before harvesting. Lymphoma cells were transfected with MYD88 or control GFP siRNA mixed in OptiMEM and RNAiMax according to the manufacturer's instructions. The mixture was added to 2×10^6 cells in 1-mL medium (2 mL total) for 6 hours, seeded into a 6-cm dish, and incubated for a further 4 days. One day before harvesting, SAHA was added to the transfected cells.

The PCMV-FLAG-WT MYD88 mutant derivatives L265P and K132R were created using oligonucleotides designed in accordance with Stratagene's QuikChange Site-Directed Mutagenesis Kit. MYD88 was identified by a loss-of-function screen as described in ref. 16.

Antibodies and compounds

The following antibodies were used: FLAG-M2 (Sigma), PARP (Cell Signaling Technology), acetylated tubulin (Sigma), actin (Sigma), HDAC6 (Millipore), phospho-Chk1 S317 (Millipore), Chk1 (Cell Signaling Technology), cleaved caspase-3 (Cell Signaling Technology), MYD88 (Cell Signaling Technology for immunoblotting and Abcam for IHC), TLR4 (Cell Signaling Technology), p53 (Santa Cruz Biotechnology), IL6 (Abcam), IL8 (Abcam), acetylated lysine (Cell Signaling Technology), and NFκB p65 (Santa Cruz Biotechnology). HDAC inhibitors were obtained from Cayman Chemical, Sigma, and Chemietek, and the MYD88 inhibitor T1617932 from AOBIOUS Inc.

Immunoblotting, immunoprecipitation, and preparation of nuclear extracts

Immunoblotting, immunoprecipitation, and nuclear extract preparation were carried out as described previously (8). Representative blots from at least three experiments are shown.

Colony formation assay and flow cytometry

U2OS-Tet-FLAG-MYD88–inducible cells were seeded at 1×10^3 cells per well in 6-well plates. FLAG-MYD88 was induced for 4 hours prior to 24 hours of drug treatment as indicated. At 9 days after drug treatment, cells were washed twice in PBS, fixed in methanol for 10 minutes, and stained with crystal violet solution for 30 minutes before extensive washing with water. The colonies were then counted. Flow cytometry was performed as described previously (16).

Reporter assay

Cells were transfected with β-galactosidase (β-gal) and Bcl-xl reporter plasmids and expressing vector as described previously (17). Triplicate samples were transferred to a 96-well plate and processed with a WinGlo 96 Microplate luminometer (Promega), and relative activity calculated according to transfection efficiency indicated by β-gal activity.

Cytokine level analysis

The levels of six cytokines, IL1β, IL12p, IL10, IL6, TNFα, and IL8, were analyzed using a cytometric bead array as described by the manufacturer (BD Biosciences).

Mass spectrometry and in-solution digest

FLAG-MYD88–stable cell lines were prepared as described previously (18, 19). Samples were digested with trypsin (0.2 μg/μL) overnight at 37°C and processed for mass spectrometry as described.

IHC pathology examination

IHC on paraffin-embedded formalin-fixed tissue was performed exactly as described previously (20).

Bioinformatics analysis and signature enrichment

A dataset of 14,816 gene signatures was created by merging signatures downloaded from http://lymphochip.nih.gov/signaturedb/ (SignatureDB), http://www.broadinstitute.org/gsea/msigdb/index.jsp MSigDB V4 (MSigDB C1–C7), http://compbio.dfci.harvard.edu/genesigdb/ Gene Signature Database V4 (GeneSigDB), UniProt Keywords (UniProtKB; refs. 21–24). Gene ontology (GO) and annotation files were downloaded from

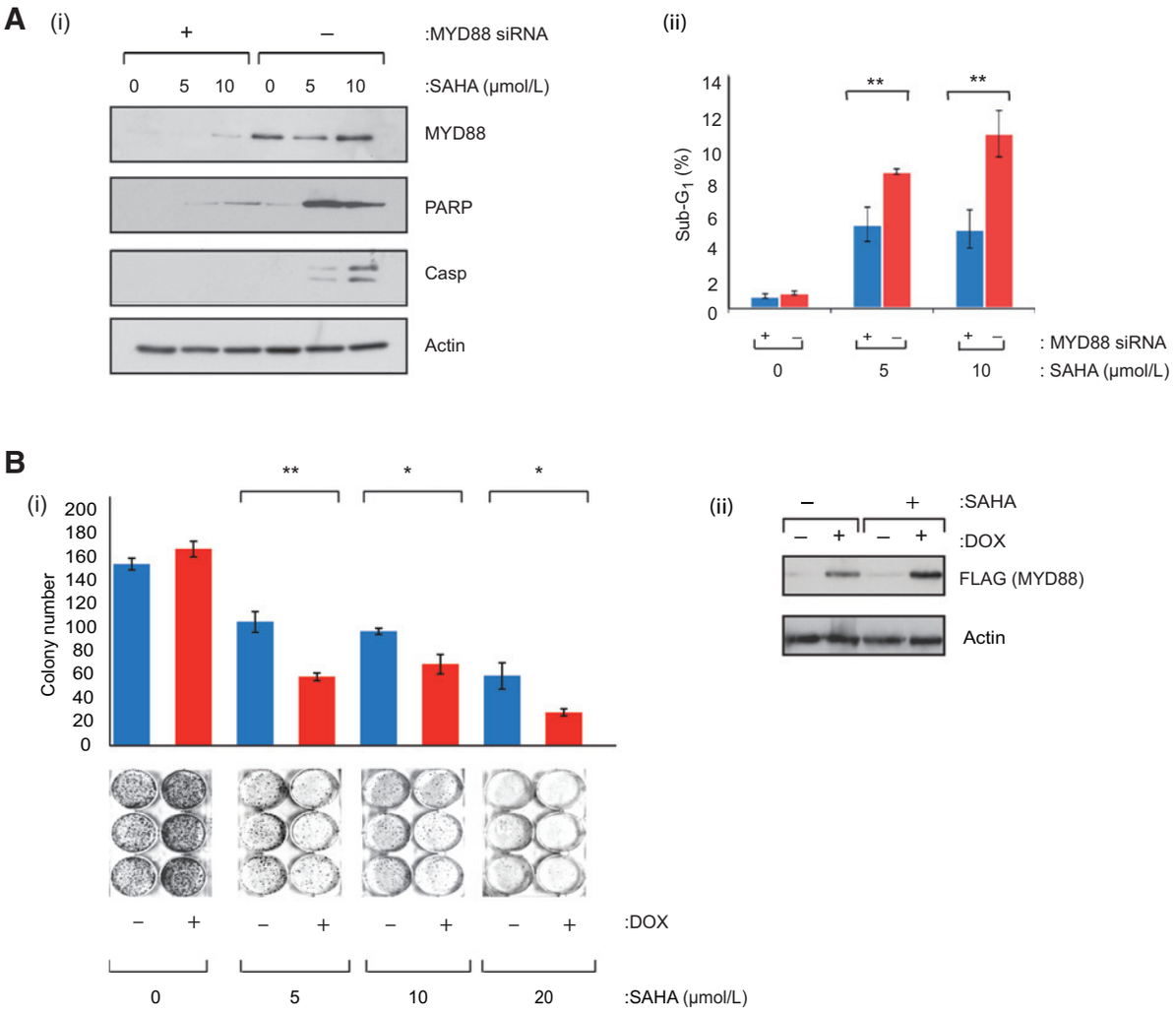

Figure 1.

MYD88 expression regulates sensitivity to HDAC inhibitors. **A, i,** U2OS cells treated with MYD88 or control (NT) siRNA (50 nmol/L for 72 hours) in the presence or absence of SAHA (5 or 10 μmol/L for 24 hours) and subsequently immunoblotted with anti-MYD88, anti-PARP (cleaved), anti-caspase-3 (cleaved), and anti-actin antibody. **ii,** U2OS cells (in triplicate) from **i** were analyzed by flow cytometry (blue bars, MYD88; red bars, NT siRNA). The sub-G_1 phase (%) is shown. Statistical significance is indicated (**, $P \leq 0.01$). **B,** U2OS cells stably expressing Tet-On inducible FLAG-tagged MYD88 were grown in triplicate in the absence (−) or presence (+) of doxycycline (DOX) together with SAHA (5, 10, or 20 μmol/L) and, after 9 days, viable cell colonies were assessed by crystal violet staining (and quantitated). The untreated control (no SAHA) cells are shown for comparison. **i,** Graphical representation with example colony stains underneath (in triplicate). Statistical significance is indicated; *, $P \leq 0.05$; **, $P \leq 0.01$. **ii,** Immunoblot of ectopic FLAG-MYD88 in the same cells as used in **i**. Note that MYD88 was one of the top seven hits in the loss-of-function screen, which ranked highly because the cells from the resistant colony contained a single shRNA and the target gene was silenced in a stable fashion in SAHA-resistant colonies.

http://www.geneontology.org (03/17/2015). The structure from the .obo and annotations from the .goa files were used to build a GO gene set. Enrichment of gene sets against signatures was assessed using a hypergeometric test, where the draw is the gene set genes, the successes are the signature genes, and the population is the number of genes present on the platform. The top 500 most MYD88-correlated genes within ABC and GC DLBCL were determined across 10 DLBCL datasets encompassing 2,030 cases (Care and colleagues; manuscript submitted). These 500 genes were used for GO and gene signature enrichment analysis.

On the basis of the top 500 in ABC DLBCL, acetylation events were assigned to the 500 genes/proteins. Annotated acetylation and acetylation sites at lysine residues of proteins (experiment based, N-terminal acetylation excluded) were obtained from the following databases: Compendium of Protein Lysine Modifications (CPML), PhosphoSite Plus, Phosida, and UniProt. On the basis of the heatmaps and the signatures, the genes in the MYD88-related ABC subgroup DLBCL nonimmune clusters were assigned to the respective clusters chr3p21/chr3p22, MCM complex/DNA unwinding, metabolic process (including pentose and organophosphate pathways), macromolecule organization, and

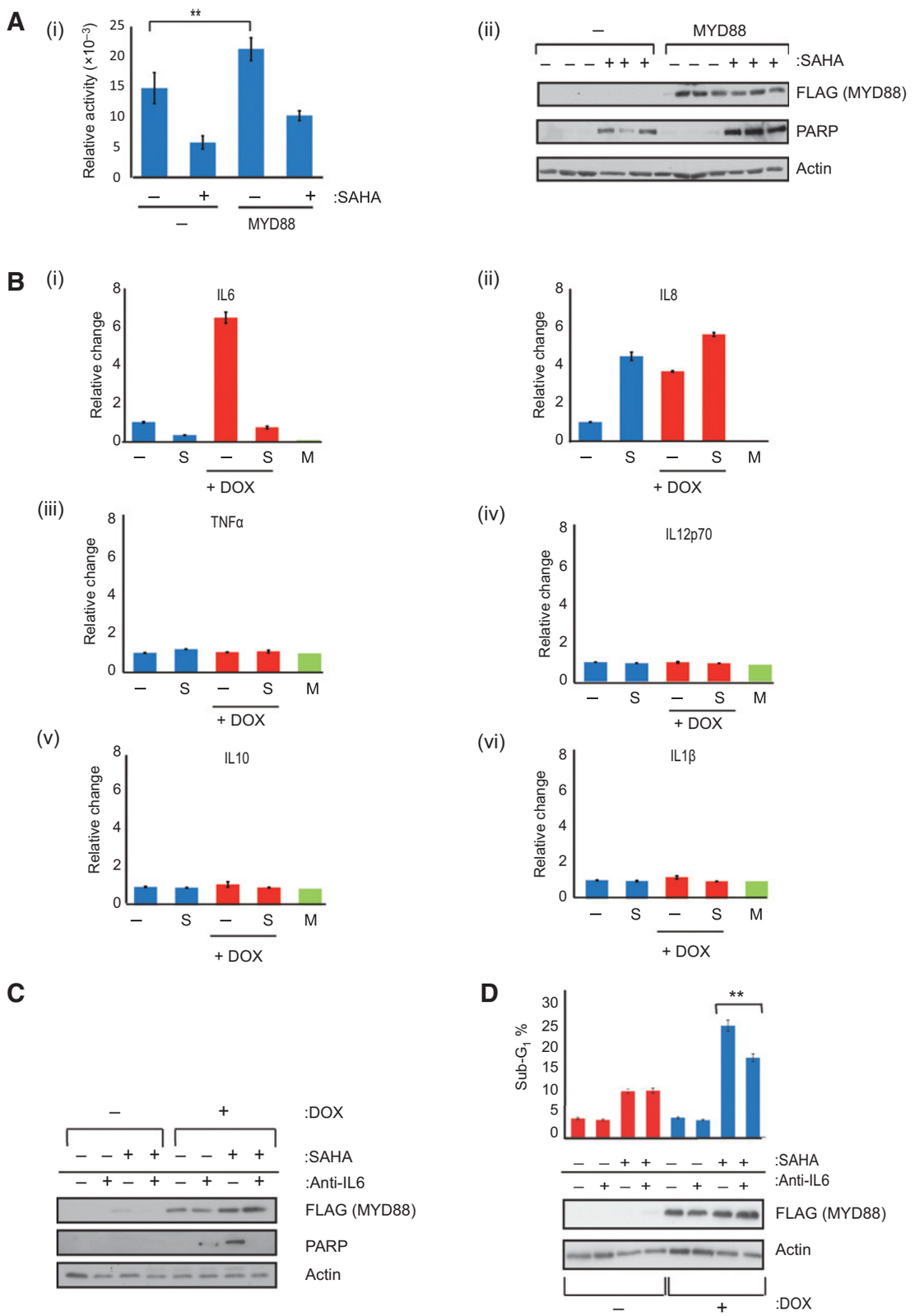
A
(i)
Relative activity (×10⁻³)
**
:SAHA
MYD88
(ii)
MYD88
:SAHA
FLAG (MYD88)
PARP
Actin
B
(i)
IL6
Relative change
+ DOX
(ii)
IL8
(iii)
TNFα
(iv)
IL12p70
(v)
IL10
(vi)
IL1β
C
:DOX
:SAHA
:Anti-IL6
FLAG (MYD88)
PARP
Actin
D
Sub-G1 %
**
:SAHA
:Anti-IL6
FLAG (MYD88)
Actin
:DOX

adhesion. Acetylation events of the genes in the different clusters were assigned and a protein list of the occurring proteins in the clusters (nonoverlapping) was compiled. The percentage of acetylation was calculated for the top 500 genes ABC DLBCL, the total number of genes from ABC DLBCL nonimmune clusters, and the individual clusters from ABC DLBCL nonimmune clusters.

Results

MYD88 expression regulates cell sensitivity to HDAC inhibitor treatment

MYD88 was identified in a genome-wide loss-of-function screen for genes that regulate cell sensitivity to HDAC inhibitors using SAHA, as described previously (16). The effect of MYD88 in regulating cell sensitivity to HDAC inhibitors was confirmed both by short-term silencing and ectopic MYD88 expression; treating cells with MYD88 siRNA reduced sensitivity to apoptosis upon SAHA treatment and conversely expressing ectopic MYD88 enhanced sensitivity to SAHA (Fig. 1A and Supplementary Fig. S1A). Furthermore, a stable inducible cell line expressing MYD88 exhibited enhanced apoptosis to SAHA (Supplementary Fig. S1B). A similar effect was observed in cell colony formation assays, where the inhibitory effect of SAHA was enhanced upon stable expression of ectopic MYD88 relative to uninduced cells (Fig. 1B). Moreover, MYD88 sensitized cells to a variety of other HDAC inhibitors, such as panobinostat, but not mechanistically unrelated agents (Supplementary Table S1). These results establish that MYD88 regulates cell sensitivity to HDAC inhibitor treatment.

Extracellular IL6 sensitizes cells to HDAC inhibition

One of the major effector arms of MYD88-dependent TLR signaling regulates cytokine gene expression, via NFκB-dependent transcription (25). To explore the mechanistic role of MYD88, we tested the impact of MYD88 on cytokine expression and thereafter the influence of cytokines on HDAC inhibitor–treated cells. The increased level of ectopic MYD88 caused the activation of NFκB and NFκB-responsive transcription (Fig. 2A and Supplementary Fig. S1C). We then measured the extracellular level of different cytokines regulated by the NFκB pathway, including IL1β, IL6, IL8, IL10, IL12, and TNFα, and observed that IL6 was elevated upon MYD88 expression and reduced by SAHA treatment (Fig. 2B). The level of IL8 was also enhanced by MYD88 but in contrast to IL6 remained high upon SAHA treatment. The effect of MYD88 expression was insignificant on the other cytokines measured under these assay conditions (Fig. 2B).

We addressed whether the increase in the level of extracellular IL6 or IL8 dependent upon MYD88 influenced cell sensitivity to HDAC inhibitors using neutralizing antibodies to inactivate IL6, which we added to the medium of cells expressing inducible ectopic MYD88 and then treated the cells with SAHA (Fig. 2C and D). We observed that the enhanced level of apoptosis (increased PARP and sub-G_1 cells) that occurred upon MYD88 expression with SAHA treatment was reduced by IL6 neutralization (Fig. 2C and D). In contrast, neutralization of IL8, under the same experimental conditions of MYD88 expression, had a modest effect on SAHA-dependent apoptosis (Supplementary Fig. S1D), suggesting that IL6 rather than IL8 is the more relevant effector in these conditions. The increased level of extracellular IL6 dependent upon MYD88 expression therefore augments cell sensitivity to HDAC inhibitors.

To explore the mechanism through which IL6 sensitizes cells to HDAC inhibitors, we considered an influence on cell-cycle progression, an idea that is consistent with previous reports describing the growth promoting effects of IL6 (26, 27). We compared MYD88- induced to uninduced cells, and noticed impaired cell-cycle progression, reflecting an increase in the size of the G_2 phase and reduced S-phase population, upon treatment with anti-IL6 antibody (25% − doxycycline to 37% + doxycycline); the anti-IL6–treated MYD88-induced cells exhibited a profile typical of cells stalled in G_2 phase (Supplementary Fig. S1E, i and ii; compare doxycycline +/− with anti-IL6 treatment). Because the cell-cycle profile was reminiscent of an active G_2 checkpoint (3, 28), we investigated whether anti-IL6–treated cells had an active G_2 checkpoint. Chk1 acts at the G_2–M phase transition in response to cellular stress (28), and S317 phosphorylation is a marker for active Chk1 kinase (3). Enhanced phosphorylation occurred at S317 upon IL6 neutralization (Supplementary Fig. S1E, iii), consistent with a role of Chk1 in the G_2 checkpoint and the increased G_2 phase cells, which appeared upon IL6 neutralization. An increase in phosphorylation at S317 also occurred in uninduced cells, although the effect in MYD88-induced cells was far more apparent (Supplementary Fig. S1E, iii). These results suggest that an effect of IL6 is to allow cell-cycle progression.

MYD88 is acetylated and deacetylated by HDAC6

Having established that MYD88 regulates cell sensitivity to HDAC inhibition, we turned our attention to the control of MYD88 activity. One possibility that we considered was a direct influence of HDAC on MYD88; for example, if MYD88 was itself acetylated. Significantly, we identified lysine acetylation on both ectopic and endogenous MYD88 protein (Fig. 3A and Supplementary Fig. S1F), and then by tandem mass spectrometry

Figure 2.

MYD88 augments IL6 levels. **A,** U2OS cells were transfected with the indicated expression vectors (1 μg) for 48 hours and treated with SAHA (10 μmol/L; +) for another 24 hours. The NFκB-responsive Bcl-xL promoter luciferase activity is shown relative to cotransfected pCMV-βgal expression (**i**), together with the level of ectopic FLAG-MYD88 protein (**ii**), PARP (cleaved), and actin, performed in triplicate. Statistical significance is indicated (**, $P \leq 0.01$). **B,** U2OS cells stably expressing Tet-On inducible FLAG-tagged MYD88 were treated with SAHA (S; 10 μmol/L) for 24 hours under noninduced or induced doxycycline (+DOX) treatment conditions (1 μg/mL; induction for 72-hour treatment), and relative levels of the indicated cytokines (IL6, IL8, TNFα, IL12p70, IL10, and IL1β) in the tissue culture media were measured using BD Cytometric Bead Array Human Inflammatory Cytokine measurement kit. The reading for preculture medium (M) is indicated. Mean values from triplicate readings. **C,** U2OS cells stably expressing Tet-On inducible FLAG-tagged MYD88 were treated with SAHA (10 μmol/L; +) and anti- IL6 neutralizing antibody (2 μg/mL) for 24 hours under noninduced (−) or induced (+) doxycycline (DOX) treatment conditions (1 μg/mL; induction for 72 hours prior to treatment). Cells were immunoblotted with anti-FLAG (for ectopic MYD88) or PARP (cleaved) and actin antibodies as indicated. Quantification indicated that cleaved PARP decreased by over 50% upon IL6 neutralization and less than 5% upon IL8 neutralization (Supplementary Fig. S1D) under conditions of MYD88 induction (+DOX) and SAHA treatment. **D,** U2OS cells stably expressing Tet-On inducible FLAG-tagged MYD88 were treated as in **C** and analyzed by flow cytometry for the level of sub-G_1 phase cells (as a percentage of the total population). Immunoblot shows the level of MYD88 (anti-FLAG) and actin. Statistical significance is indicated as **, $P \leq 0.01$.

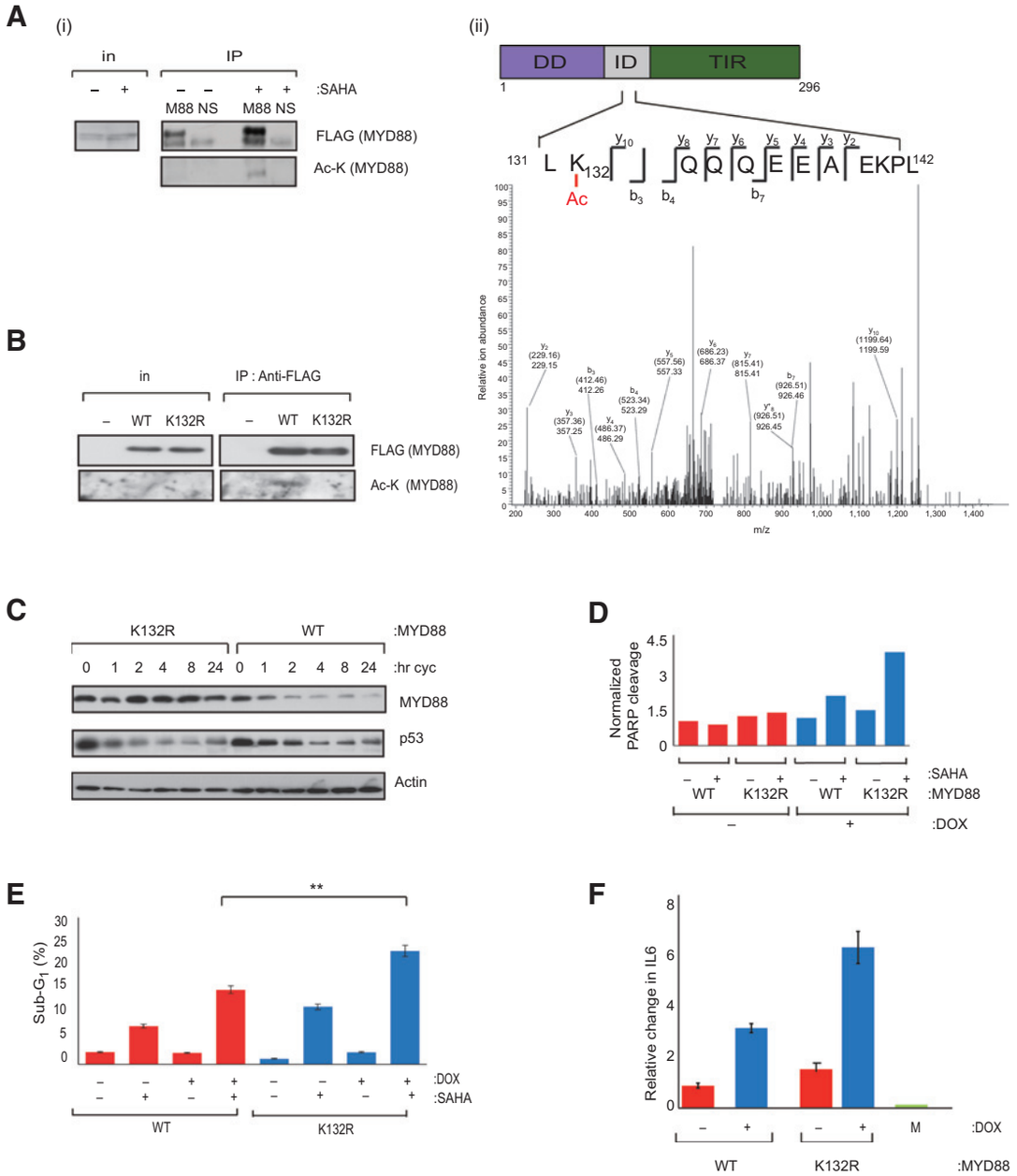

Figure 3.

MYD88 is acetylated. **A, i,** Cells stably expressing FLAG-MYD88 were treated with SAHA (+; 10 μmol/L) for 16 hours and immunoprecipitated with FLAG (M88) or nonspecific (NS) antibody prior to immunoblotting with MYD88 and acetyl-lysine antibody (Ac-K). Input (2%) level of MYD88 is shown. A 10% increase in the acetylation level of MYD88 occurred in SAHA-treated cells. **ii,** Domain organization of MYD88. DD, death domain; ID, intermediate domain; TIR, Toll-like receptor interacting domain. MYD88 was immunopurified as described in **A** and analyzed by mass spectrometry. The MS/MS spectrum of the peptide 131LKQQQEEAEKPL142 derived from MYD88 (SwissProt no Q99836) demonstrates acetylation at lysine (K) 132. B and y fragment ions are indicated. **B,** FLAG-MYD88 WT, FLAG-K132R, or control (−) inducible U2OS cell lines were induced for 2 days with doxycycline (DOX). Cells were harvested and MYD88 or its mutant immunoprecipitated with anti-FLAG antibody and immunoblotted with anti-FLAG or anti-acetyl-lysine antibody. Input is indicated (inset). **C,** Stable U2OS cells expressing Tet-On inducible WT or K132R FLAG-MYD88 were treated with cycloheximide (100 μmol/L) for the indicated time and immunoblotted with FLAG, p53, and actin antibody. Immunoblot quantitation of FLAG-MYD88 relative to actin performed using ImageJ software; WT and K132R had a half-life of 2 and 8 hours, respectively. **D,** Stable Tet-On inducible U2OS cell lines expressing WT or K132R FLAG-MYD88 were treated with SAHA (10μmol/L) for 16 hours under noninduced (−) or induced (+) doxycycline (DOX) treatment conditions (1 μg/mL; induction for 72 hours prior to treatment). Cells were immunoblotted for MYD88 (anti-FLAG), PARP (cleaved), and actin antibody. The graph represents quantitation of PARP cleavage. **E,** Level of sub-G_1 in stable Tet-On inducible U2OS cell lines expressing WT or K132R FLAG-MYD88 U2OS under noninduced (−) or induced (+) doxycycline (DOX) treatment conditions by flow cytometry, upon SAHA treatment (10 μmol/L) for 16 hours, as described in **D**. Statistical significance is indicated as **, $P \leq 0.01$. **F,** Relative level of IL6 in tissue culture medium was measured using BD Cytometric Bead Array Human Inflammatory Cytokine Kit. Mean values from triplicate readings are shown in U2OS cells stably expressing Tet-On inducible WT or K132R MYD88 under non-induced (-) or induced (+) doxycycline (DOX) treatment conditions (1 μg/mL; induction for 72-hour treatment), as described in **D**.

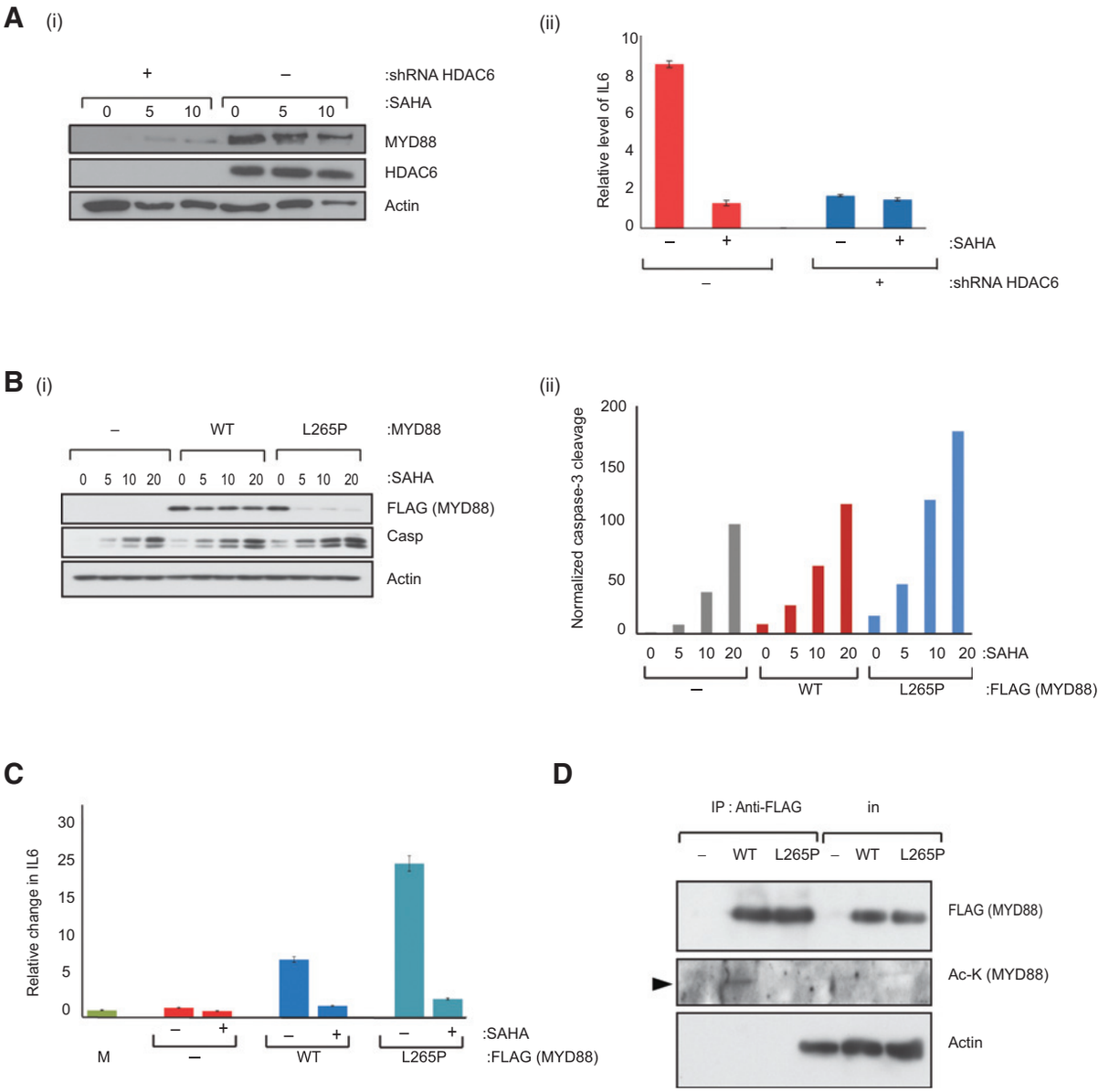

Figure 4.

Properties of MYD88. **A, i,** Control (−) and HDAC6 knockdown (+; stable shRNA knockdown) U2OS cells were treated with SAHA at the indicated concentrations for 24 hours and analyzed by immunoblotting for HDAC6 and MYD88. Actin was the loading control. **ii,** Relative levels of IL6 in tissue culture medium were measured using BD Cytometric Bead Array Kit. Mean values from triplicate readings are shown in U2OS control (−) and HDAC6 knockdown (+; stable shRNA knockdown) cells. **B, i,** U2OS cells were transfected with empty vector (−), FLAG-MYD88 (WT), or FLAG-L265P. SAHA (5, 10, or 20 μmol/L) or DMSO (0) was added, and 24 hours later, cells were immunoblotted with FLAG, caspase-3 (cleaved), or actin antibodies. The reduced level of L265P in SAHA-treated cells was reproducibly observed in at least three independent experiments; the reasons for the reduction remain unclear. **ii,** Graph represents the quantitated caspase-3 (cleaved) from **C** (**i**), normalized to actin loading control using ImageJ software. **C**, Relative levels of IL6 in tissue culture medium (M) measured using BD Cytometric Bead Array Kit. Mean values from triplicate readings are shown in U2OS expressing WT or L265P MYD88 in the presence or absence of SAHA treatment (5 μmol/L). **D,** U2OS cells were transfected with empty vector, FLAG-MYD88 (WT), or FLAG-L265P. Cells were harvested and immunoprecipitated with anti-FLAG and immunoblotted with anti-FLAG or anti-acetyl-lysine (Ac-K) antibody. Input levels are indicated, together with acetylated MYD88.

identified a single acetylated lysine (K) residue (K132; Fig. 3A). Furthermore, the low but detectable acetylation level on MYD88 contrasted with its mutant derivative, carrying a lysine to arginine substitution (K132R), which showed reduced acetylation (Fig. 3B), suggesting that K132R is an acetylation loss-of-function mutant. Most importantly, K132R exhibited a longer half-life relative to wild-type MYD88 (Fig. 3C), suggesting that acetylation influenced the stability of MYD88. We then compared the properties of wild-type MYD88 to K132R, beginning with HDAC inhibitor sensitivity and observed that K132R expression

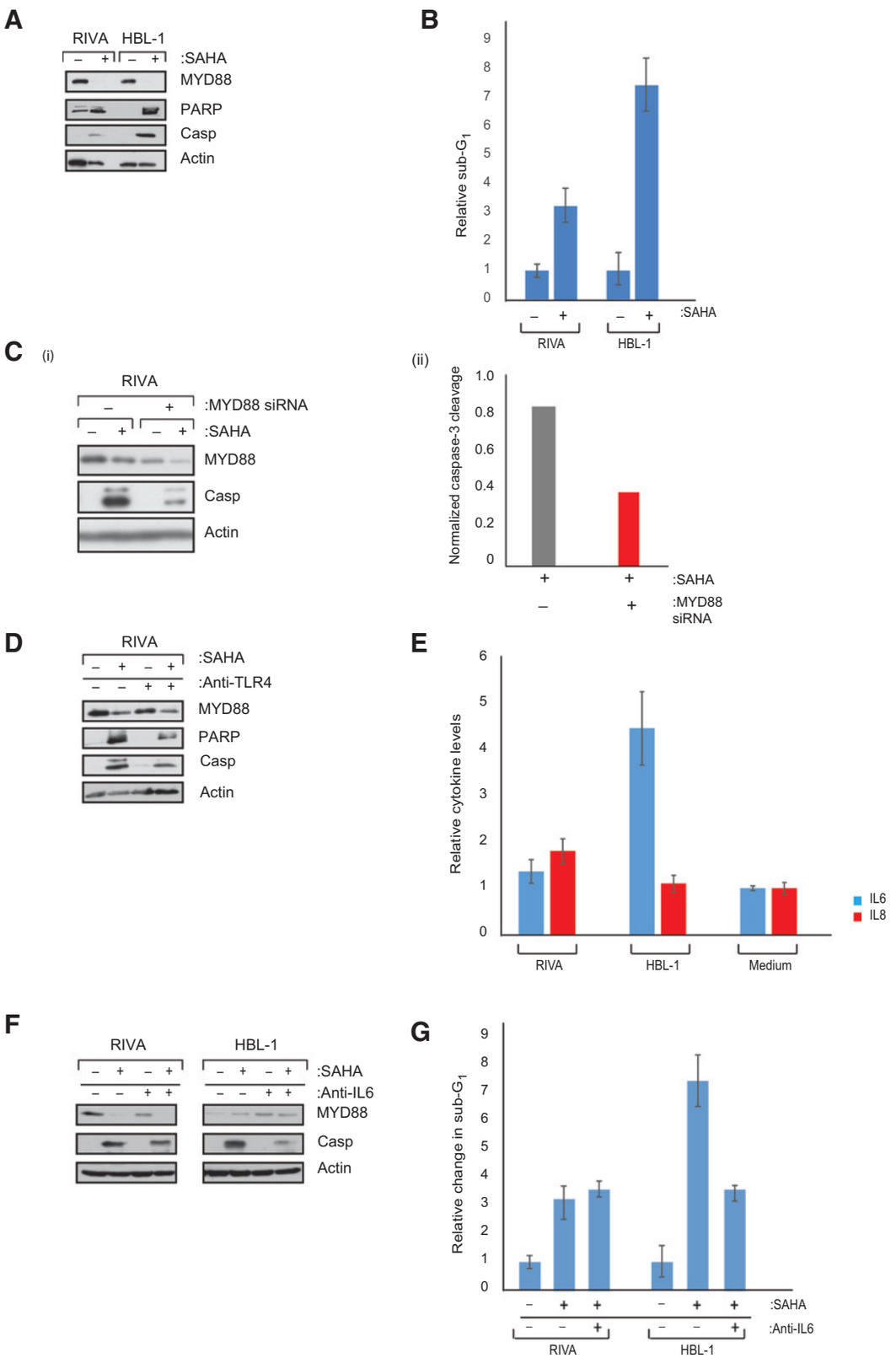
A
RIVA
HBL-1
:SAHA
MYD88
PARP
Casp
Actin
B
Relative sub-G1
:SAHA
RIVA
HBL-1
C
(i)
RIVA
:MYD88 siRNA
:SAHA
MYD88
Casp
Actin
(ii)
Normalized caspase-3 cleavage
:SAHA
:MYD88 siRNA
D
RIVA
:SAHA
:Anti-TLR4
MYD88
PARP
Casp
Actin
E
Relative cytokine levels
IL6
IL8
RIVA
HBL-1
Medium
F
RIVA
HBL-1
:SAHA
:Anti-IL6
MYD88
Casp
Actin
G
Relative change in sub-G1
:SAHA
:Anti-IL6
RIVA
HBL-1

sensitized cells to a higher level of apoptosis upon HDAC inhibitor treatment compared with wild-type MYD88 (PARP cleavage and sub-G_1 cells; Fig. 3D and E). Furthermore, the heightened effect of K132R coincided with an increased extracellular IL6 level compared with wild-type MYD88 (Fig. 3F). MYD88 is thus a direct target for acetylation, and acetylation impacts on its biochemical and biological properties.

We considered HDAC6 as a possible deacetylase, given its cytoplasmic colocalization with MYD88 and role in regulating cytoplasmic substrates (29), and assessed the effect of silencing HDAC6 on MYD88. We observed in HDAC6-depleted cells a reduced level of MYD88 and concomitant reduction in IL6 (Fig. 4A and Supplementary Fig. S2A–S2C). Furthermore, in cells treated with tubastatin A, a small-molecule inhibitor of HDAC6 (30), MYD88 levels were also reduced (Supplementary Fig. S2B and S2C); the acetylation of tubulin, a recognized substrate of HDAC6 (31), increased under tubastatin A treatment (Supplementary Fig. S2C). Overall, the results highlight HDAC6 as a key regulator of MYD88 and more generally suggest that acetylation controls the activity of MYD88.

Somatic mutation in MYD88 influences HDAC inhibitor sensitivity

MYD88 is expressed at high levels in the hematopoietic lineage and somatic mutation in MYD88, resulting in the L265P substitution observed in the ABC subtype of DLBCL and frequently in Waldenstrom macroglobulinemia (14, 15). L265P is believed to result in an oncogenic gain-of-function mutation, which augments signaling through NFκB (14). We reasoned therefore that L265P may impact on MYD88 as a sensitizer to HDAC inhibitor treatment. When the effect of L265P was compared with wild-type MYD88, an enhanced level of apoptosis was apparent upon HDAC inhibitor treatment and increased IL6 production was evident (Fig. 4B and C). Furthermore, L265P displayed a lower level of acetylation compared with its wild-type counterpart (Fig. 4D).

To establish the importance of the results for lymphoma cells, we used two pathologically relevant ABC-like DLBCL cell lines, RIVA and HBL-1, representing either wild-type MYD88 (RIVA) or a heterozygous somatic L265P mutation, respectively. We found that HBL-1 cells, expressing heterozygous MYD88 L265P, were more sensitive than RIVA cells to apoptosis (Fig. 5A and B). Moreover, the apoptosis seen upon HDAC inhibitor treatment required MYD88, as depleting MYD88 in RIVA cells reduced cell sensitivity to SAHA treatment (Fig. 5C) and TLR signaling, as treating cells with an anti-TLR4 antibody, which blocks TLR signaling (32), reduced the level of apoptosis (Fig. 5D). We then examined the level of cytokine production by each cell line and observed that extracellular IL6 was higher in HBL-1 compared with RIVA cells, in contrast to IL8 (Fig. 5E). Furthermore, neutralizing extracellular IL6 with anti-IL6 antibody caused a reduction in HDAC inhibitor–induced apoptosis (caspase-3 cleavage and sub-G_1 cells) in HBL-1 compared with RIVA cells (Fig. 5F and G), and conversely treatment with lipopolysaccharide (LPS) to augment extracellular cytokine levels increased sensitivity to SAHA treatment (Supplementary Fig. S2D and S2E). Moreover, taking a chemical biology approach to inactivate MYD88 using the small-molecule MYD88 dimerization inhibitor T6167923 (33) on cells treated with LPS caused a significant reduction in the level of SAHA-induced apoptosis (Supplementary Fig. S2D). Altogether, these results suggest that MYD88, by virtue of its ability to act through TLR signaling and augment extracellular IL6 levels, regulates cell sensitivity to HDAC inhibition.

We also examined by IHC MYD88 expression in tissue microarray biopsies from patients with DLBCL compared with biopsies taken from patients with prostate and colorectal cancer, and noncancerous tonsillar tissue biopsies; Waldenstrom macroglobulinemia sections stained for MYD88 served as a positive control (Supplementary Fig. S3). High levels of MYD88 were apparent in the DLBCL sections, but not prostate and colorectal cancer (Supplementary Fig. S3A–S3E). The conclusions drawn from the cell-based studies relating to the role of MYD88 in lymphoma cell lines could therefore be relevant to the clinical disease.

MYD88 expression coincides with an acetylation signature

As MYD88 is believed to be important in the pathology of the ABC subgroup of DLBCL (14) and because MYD88 confers cell sensitivity to HDAC inhibitors, we reasoned that there might be a group of genes whose expression coincided with MYD88, that were functionally related with the role of MYD88 in HDAC inhibition. We thus took a bioinformatics approach to determine at the genome-wide level whether a gene signature correlated with MYD88 expression by interrogating gene expression datasets derived from DLBCL clinical biopsies. Accordingly, we ranked the 500 most correlated genes with MYD88 expression and clustered them according to GO descriptors (Fig. 6A). There was some overlap between the GO clusters within the ABC and GC subgroups, mostly related to immunologic GO terms and therefore likely to reflect a shared signature of host immune response (Fig. 6A and Supplementary Fig. S4). Notably, a number of ABC subgroup–specific GO gene clusters were apparent (Fig. 6A, bottom right square); for example, the MCM complex/DNA

Figure 5.

Sensitivity of DLBCL cell lines to HDAC inhibitors. **A,** RIVA and HBL-1 cells were treated with SAHA (5 μmol/L) for 24 hours prior to immunoblotting with anti-MYD88, PARP (cleaved), caspase-3 (cleaved), and actin antibody. The IC_{50} of SAHA was 2.3 μmol/L for RIVA cells and 1.8 μmol/L for HBL-1 cells. **B,** RIVA and HBL-1 cells were either untreated (−) or treated with SAHA (5 μmol/L; +) for 24 hours and analyzed by flow cytometry. The level of sub-G_1 cells is shown, normalized to the basal level of sub-G_1 in untreated cells. Mean with SEs based on three different experiments. **C, i,** RIVA cells were treated with MYD88 or control (GFP) siRNA for 96 hours and either untreated (−) or treated with SAHA (5 μmol/L; +) for 24 hours before immunoblotting with anti-MYD88, anti-caspase-3 (cleaved) and anti-actin antibody. **ii,** The graph represents the quantitated level of caspase-3 (cleaved) from **C** (**i**) upon SAHA treatment (+) normalized to actin using ImageJ software. **D,** RIVA cells were grown in medium containing an anti-TLR4 antibody for 4 hours and then treated with SAHA (5 μmol/L) for 24 hours, and immunoblotted with anti-MYD88, PARP (cleaved), caspase-3 (cleaved), and actin. **E**, Relative levels of IL6 (blue) and IL8 (red), normalized to the background level in medium alone, detected in the tissue culture medium of RIVA and HBL-1 cells were measured using BD Cytometric Bead Array Human Inflammatory Cytokine measurement kit. Mean with SEs based on three different experiments is shown. The mean absolute cytokine readings were RIVA IL6, 13.1 pg/mL; IL8, 76.8 pg/mL; HBL-1 IL6, 79.9 pg/mL; IL8, 38.8 pg/mL. **F,** RIVA and HBL-1 cells were treated with SAHA (5 μmol/L) and IL6-neutralizing antibody for 24 hours as indicated and then immunoblotted with anti-MYD88, caspase-3 (cleaved), and actin antibody. **G,** RIVA and HBL-1 cells were treated as described in **F** and analyzed by flow cytometry. The level of sub-G_1 cells is shown, normalized to the basal level of sub-G_1 in untreated cells. Mean with SEs based on three different experiments.

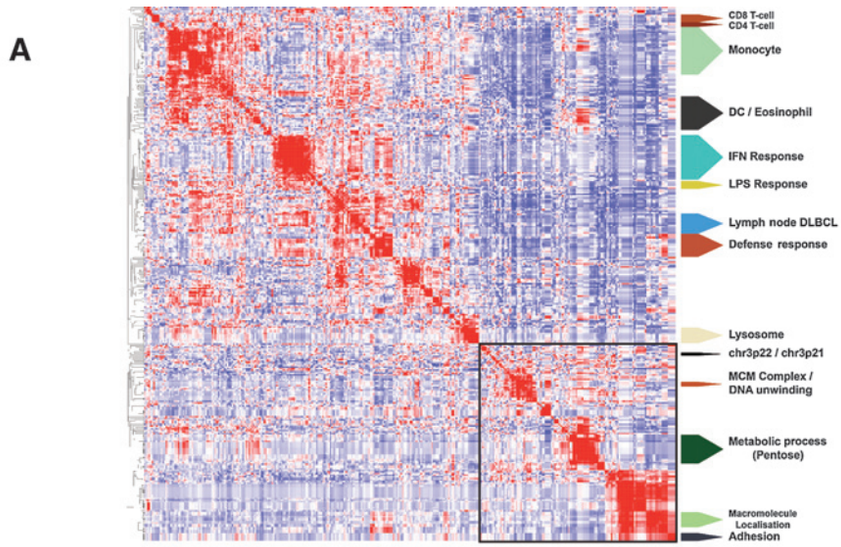
A
CD8 T-cell
CD4 T-cell
Monocyte
DC / Eosinophil
IFN Response
LPS Response
Lymph node DLBCL
Defense response
Lysosome
chr3p22 / chr3p21
MCM Complex /
DNA unwinding
Metabolic process
(Pentose)
Macromolecule
Localisation
Adhesion

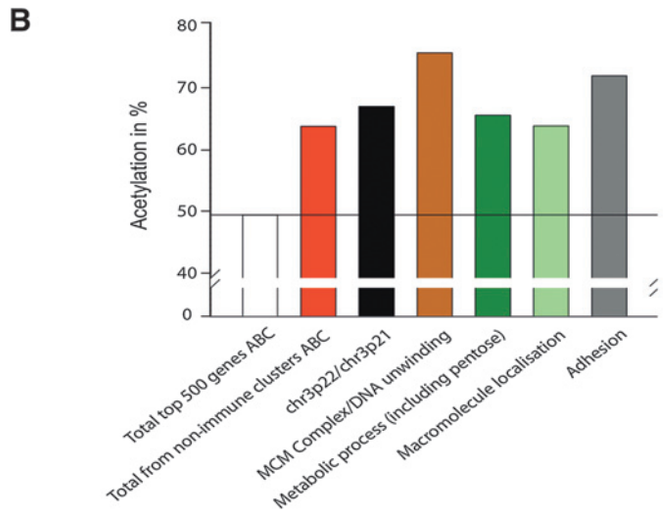
B
Acetylation in %
80
70
60
50
40
0
Total top 500 genes ABC
Total from non-immune clusters ABC
chr3p22/chr3p21
MCM Complex/DNA unwinding
Metabolic process (including pentose)
Macromolecule localisation
Adhesion

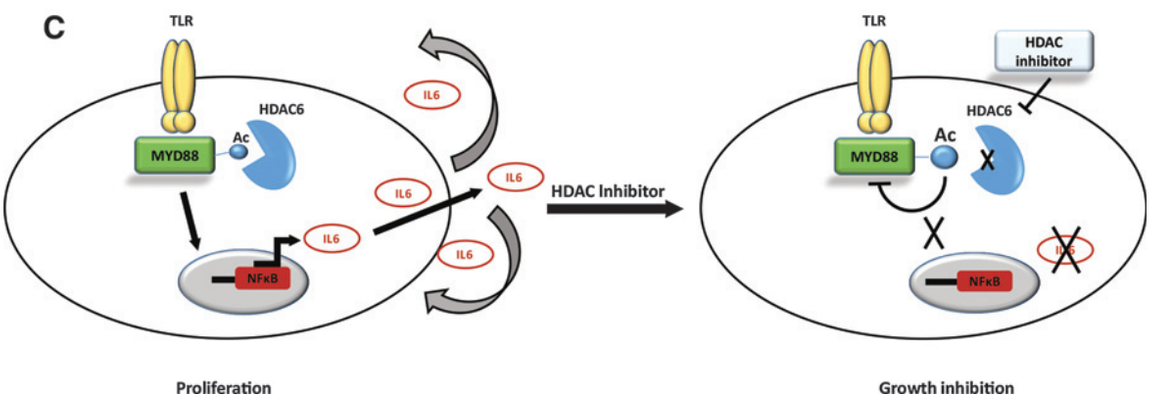
C
TLR
HDAC6
Ac
MYD88
NFκB
IL6
HDAC Inhibitor
HDAC
inhibitor
Proliferation
Growth inhibition

unwinding and metabolic process GO terms. Because some of the genes in these GO clusters are known to encode lysine acetylation targets, we examined in greater detail the acetylation content of each cluster. This indicated that each ABC subgroup–specific cluster had a high content of lysine acetylation targets, above the average lysine acetylation content of the top 500 genes (Fig. 6B). Thus, in the ABC subgroup, MYD88 expression is associated with an enriched set of genes, which, in addition to their GO term, are related through their high level of lysine acetylation.

Discussion

MYD88 is an essential cytosolic adaptor protein expressed at high levels in the hematopoietic lineage, required for signaling induced by members of the TLR and IL1R super family, which play an important role in innate and adaptive immunity by regulating the expression of diverse proinflammatory genes through the activation of NFκB (25, 34). Somatic mutation in MYD88 resulting in L265P has been described in a number of human hematologic malignancies, including the ABC subtype of DLBCL and Waldenstrom macroglobulinemia (14, 15). The L265P mutation is believed to provide a gain-of-function, which activates MYD88-dependent TLR signaling, thereby driving NFκB activity and inflammatory gene expression (14).

We identified MYD88 through an unbiased loss-of-function screen aiming to define cellular pathways that are responsible for growth inhibition by HDAC inhibitors, as described previously (16). The screen identifies genes that, when expressed, sensitize cells to drug-induced cell death (8, 20). As MYD88 is a mediator of inflammatory signaling, we assessed the role of cytokines, and found that increased levels of extracellular IL6 are an important downstream effector of HDAC inhibitor cell sensitivity. The fact that neutralization of extracellular IL6 reduced the effect of HDAC inhibitors on cells provides a direct test for the autocrine action of IL6 in mediating cell sensitivity to HDAC inhibitors.

Our results suggest that one role of the pleiotropic cytokine IL6 (26, 27) is to enable cell-cycle progression by allowing transition through the G_2 phase checkpoint (28, 35), which is significant because, at a general level, HDAC inhibitors affect proliferating cells more so than nonproliferating cells (9). Cells expressing MYD88 with an active TLR signaling pathway are therefore likely to exhibit increased sensitivity to HDAC inhibitors (Fig. 6C).

We identified an acetylation site at residue K132. The K132R-mutant derivative exhibited increased protein stability and caused higher levels of IL6 and apoptosis relative to wild-type MYD88, establishing a mechanistic connection between MYD88 acetylation and cytokine signaling. We further identified HDAC6 as a key upstream regulator of MYD88 acetylation, which in turn enables HDAC and HDAC inhibitors, which target HDAC6 to impact on MYD88 activity. The reduced level of MYD88 in HDAC6-depleted cells is entirely consistent with the observed increase in half-life of the hypoacetylated K132R mutant, arguing that deacetylation by HDAC6 endows MYD88 with enhanced signaling capability (Fig. 6C). Furthermore, HDAC inhibitors influence innate immunity and have immune-modulating functions (36–39). Consequently, our results detailing the acetylation of MYD88 provide a possible mechanism that relates HDAC inhibition to immune modulation.

It is of further interest that MYD88 undergoes somatic mutation in DLBCL and Waldenstrom macroglobulinemia (14, 15, 40), and our results suggest that L265P impacts on the sensitivity of the malignant cells to HDAC inhibitors. The increased sensitivity of cells expressing L265P could reflect the ability of IL6 to promote proliferation, as documented in the cell systems investigated in this study, and is consistent with high level production of IL6 by DLBCL and Waldenstrom macroglobulinemia in clinical disease (14, 41). It will be interesting to assess how the ABC subgroup in general, and specifically the L265P subgroup, responds to HDAC inhibitor-based therapeutics. Furthermore, MYD88 has been implicated in other malignancies, for example, metastatic hepatocellular carcinoma (42), where it will be important to establish its role in mediating the effect of HDAC inhibitors in the pathology.

We uncovered a provocative relationship involving MYD88 acetylation, where MYD88 expression in the ABC subgroup correlated with a subgroup-specific cluster of genes, which exhibit distinct ontological relationships relative to the GC subgroup. Most importantly, an analysis of each GO cluster indicated a high representation of genes encoding lysine acetylation targets. Thus MYD88, which is itself subject to acetylation control, is a representative of a broader network of genes that share a propensity to encode proteins subject to acetylation control, perhaps suggestive of a more general role for lysine acetylation in mechanisms relevant to the ABC subgroup.

In conclusion, our study highlights a novel mechanism through which MYD88 and its role as an adaptor protein in TLR signaling regulate cell sensitivity to HDAC inhibitors, in part, mediated through the expression and autocrine action of cytokines like IL6 (Fig. 6C). We suggest that the ability of IL6 to foster cellular proliferation thereby augments cell sensitivity to HDAC inhibitor treatment. Most importantly, the mechanism is likely to be relevant to the established sensitivity of hematologic malignancies to HDAC inhibitors (10) and argues in addition that

Figure 6.

MYD88 is in an acetylation signature. **A,** The top gene signatures and GO terms enriched for the 500 most MYD88-correlated genes in ABC DLBCL ($n = 346$ signatures). The black box surrounds a subset of nonimmune–related signatures specific to the ABC subgroup ($n = 127$). The heatmap is clustered according to the correlation of the genes contributing to term enrichments. To the right of each heatmap, general categories corresponding to major correlation clusters are illustrated. A high resolution version of the heatmap is available in Supplementary Fig. S5. **B,** Graph representing the lysine acetylation content (as a percentage) of each nonimmune GO gene cluster reflecting the term enrichments in **A**, compared with the lysine acetylation content of total top 500 genes and total non immune –related clusters. Colored bars correspond to the nonimmune GO terms in **A**. **C,** Model depicting the role of MYD88 as a sensitizer to HDAC inhibitor treatment. It is envisaged, through its role as an adaptor protein in TLR-dependent signaling, that in untreated lymphoma cells (left-hand diagram), MYD88 augments NFκB activity, which thereby increases the expression of target genes, including cytokine genes like IL6. The autocrine action of IL6 retains cells in the proliferative state and augments cell sensitivity to HDAC inhibitors. Acetylated MYD88 is deacetylated by HDAC6. Upon treating cells with HDAC inhibitor (right), increased acetylation of MYD88 occurs, resulting in reduced MYD88 and NFκB activity, lowering IL6 expression and thereby prompting growth inhibition through reduced IL6 levels. It is suggested that altered MYD88 acetylation contributes to the antiproliferative effects of HDAC inhibitor treatment by preventing the autocrine growth-promoting action of cytokines like IL6.

inflammatory disease where MYD88 expression is high might also be susceptible to HDAC inhibitor–based therapies. Our results therefore establish the importance of TLR signaling and innate immunity, and more generally the inflammatory properties of the extracellular tumor microenvironment, in mediating the effect of HDAC inhibitors on malignant cells.

Disclosure of Potential Conflicts of Interest

No potential conflicts of interest were disclosed.

Authors' Contributions

Conception and design: M. New, M. Bekheet, H. Olzscha, S. Fotheringham, N.B. La Thangue

Development of methodology: M. New, S. Sheikh, M. Bekheet, H. Olzscha, S. Fotheringham, N.B. La Thangue

Acquisition of data (provided animals, acquired and managed patients, provided facilities, etc.): M. New, S. Sheikh, M. Bekheet, H. Olzscha, M.-L. Thezenas, B.M. Kessler, N.B. La Thangue

Analysis and interpretation of data (e.g., statistical analysis, biostatistics, computational analysis): M. New, S. Sheikh, M. Bekheet, H. Olzscha, M.-L. Thezenas, M.A. Care, R.M. Tooze, B.M. Kessler, N.B. La Thangue

Writing, review, and/or revision of the manuscript: M. New, S. Sheikh, M. Bekheet, H. Olzscha, R.M. Tooze, B.M. Kessler, N.B. La Thangue

Administrative, technical, or material support (i.e., reporting or organizing data, constructing databases): M. New, H. Olzscha, N.B. La Thangue

Study supervision: M. New, N.B. La Thangue

Acknowledgments

The authors thank the MRC, CRUK, and Rosetrees Trust for supporting this work.

Grant Support

This work was supported by the MRC, CRUK (Programme grantC300/A13058), and Rosetrees Trust. M. New was in receipt of a Gordon Pillar studentship from LLR, S. Sheikh an Anya Sturdy Fellowship and a CRUK Clinical Research Fellowship, M. Bekheet a Yousef Jameel Fellowship, and H. Olzscha a long-term EMBO Fellowship.

The costs of publication of this article were defrayed in part by the payment of page charges. This article must therefore be hereby marked advertisement in accordance with 18 U.S.C. Section 1734 solely to indicate this fact.

Received February 26, 2016; revised August 22, 2016; accepted September 20, 2016; published OnlineFirst October 12, 2016.

References

1. Dawson MA, Kouzarides T, Huntly BJ. Targeting epigenetic readers in cancer. N Engl J Med 2012;367:647–57.
2. Finley A, Copeland RA. Small molecule control of chromatin remodeling. Chem Biol 2014;21:1196–210.
3. Wilsker D, Petermann E, Helleday T, Bunz F. Essential function of Chk1 can be uncoupled from DNA damage checkpoint and replication control. Proc Natl Acad Sci U S A 2008;105:20752–57.
4. Choudhary C, Kumar C, Gnad F, Nielsen ML, Rehman M, Walther TC, et al. Lysine acetylation targets protein complexes and co-regulates major cellular functions. Science 2009;325:834–40.
5. Choudhary C, Weinert BT, Nishida Y, Verdin E, Mann M. The growing landscape of lysine acetylation links metabolism and cell signalling. Nat Rev Mol Cell Biol 2014;15:536–50.
6. Stimson L, Wood V, Khan O, Fotheringham S, La Thangue NB. HDAC inhibitor-based therapies and haematological malignancy. Ann Oncol 2009;20:1293–302.
7. Dawson MA, Kouzarides T. Cancer epigenetics: from mechanism to therapy. Cell 2012;150:12–27.
8. New M, Olzscha H, La Thangue NB. HDAC inhibitor-based therapies: can we interpret the code? Mol Oncol 2012;6:637–56.
9. Reichert N, Choukrallah MA, Matthias P. Multiple roles of class I HDACs in proliferation, differentiation, and development. Cell Mol Life Sci 2012;69:2173–87.
10. Falkenberg KJ, Johnstone RW. Histone deacetylases and their inhibitors in cancer, neurological diseases and immune disorders. Nat Rev Drug Discov 2014;13:673–91.
11. Dokmanovic M, Clarke C, Marks PA. Histone deacetylase inhibitors: overview and perspectives. Mol Cancer Res 2007;5:981–9.
12. Marks PA. Discovery and development of SAHA as an anticancer agent. Oncogene 2007;26:1351–6.
13. San-Miguel JF, Hungria VT, Yoon SS, Beksac M, Dimopoulos MA, Elghandour A, et al. Panobinostat plus bortezomib and dexamethasone versus placebo plus bortezomib and dexamethasone in patients with relapsed or relapsed and refractory multiple myeloma: a multicentre, randomised, double-blind phase 3 trial. Lancet Oncol 2014;15:1195–206.
14. Ngo VN, Young RM, Schmitz R, Jhavar S, Xiao W, Lim KH, et al. Oncogenically active MYD88 mutations in human lymphoma. Nature 2011;470:115–9.
15. Treon SP, Xu L, Yang G, Zhou Y, Liu X, Cao Y, et al. MYD88 L265P somatic mutation in Waldenstrom's macroglobulinemia. N Engl J Med 2012;367:826–33.
16. Fotheringham S, Epping MT, Stimson L, Khan O, Wood V, Pezzella F, et al. Genome-wide loss-of-function screen reveals an important role for the proteasome in HDAC inhibitor-induced apoptosis. Cancer Cell 2009;15:57–66.
17. Zheng SS, Moehlenbrink J, Lu YC, Zalmas LP, Sagum CA, Carr S, et al. Arginine methylation-dependent reader-writer interplay governs growth control by E2F-1. Mol Cell 2013;52:37–51.
18. Fischer R, Trudgian DC, Wright C, Thomas G, Bradbury LA, Brown MA, et al. Discovery of candidate serum proteomic and metabolomic biomarkers in ankylosing spondylitis. Mol Cell Proteomics 2012;11:M111 013904.
19. Cho EC, Zheng S, Munro S, Liu G, Carr SM, Moehlenbrink J, et al. Arginine methylation controls growth regulation by E2F-1. EMBO J 2012;31:1785–97.
20. Khan O, Fotheringham S, Wood V, Stimson L, Zhang C, Pezzella F, et al. HR23B is a biomarker for tumor sensitivity to HDAC inhibitor-based therapy. Proc Natl Acad Sci U S A 2010;107:6532–7.
21. Culhane AC, Schwarzl T, Sultana R, Picard KC, Picard SC, Lu TH, et al. GeneSigDB-a curated database of gene expression signatures. Nucleic Acids Res 2010;38:D716–D25.
22. Monti S, Savage KJ, Kutok JL, Feuerhake F, Kurtin P, Mihm M, et al. Molecular profiling of diffuse large B-cell lymphoma identifies robust subtypes including one characterized by host inflammatory response. Blood 2005;105:1851–61.
23. Shaffer AL, Wright G, Yang LM, Powell J, Ngo V, Lamy L, et al. A library of gene expression signatures to illuminate normal and pathological lymphoid biology. Immunol Rev 2006;210:67–85.
24. Subramanian A, Tamayo P, Mootha VK, Mukherjee S, Ebert BL, Gillette MA, et al. Gene set enrichment analysis: a knowledge-based approach for interpreting genome-wide expression profiles. Proc Natl Acad Sci U S A 2005;102:15545–50.
25. Takeda K, Akira S. TLR signaling pathways. Sem Immunol 2004;16:3–9.
26. Hodge DR, Hurt EM, Farrar WL. The role of IL-6 and STAT3 in inflammation and cancer. Eur J Cancer 2005;41:2502–12.
27. Chang Q, Daly L, Bromberg J. The IL-6 feed-forward loop: a driver of tumorigenesis. Sem Immunol 2014;26:48–53.
28. Liu QH, Guntuku S, Cui XS, Matsuoka S, Cortez D, Tamai K, et al. Chk1 is an essential kinase that is regulated by Atr and required for the G(2)/M DNA damage checkpoint. Gene Dev 2000;14:1448–59.
29. Into T, Inomata M, Niida S, Murakami Y, Shibata K. Regulation of MyD88 aggregation and the MyD88-dependent signaling pathway by sequestosome 1 and histone deacetylase 6. J Biol Chem 2010;285:35759–69.
30. Butler KV, Kalin J, Brochier C, Vistoli G, Langley B, Kozikowski AP. Rational design and simple chemistry yield a superior, neuroprotective HDAC6 inhibitor, tubastatin A. J Am Chem Soc 2010;132:10842–6.

31. Valenzuela-Fernandez A, Cabrero JR, Serrador JM, Sanchez-Madrid F. HDAC6: a key regulator of cytoskeleton, cell migration and cell-cell interactions. Trends Cell Biol 2008;18:291–7.
32. Tomchuck SL, Zwezdaryk KJ, Coffelt SB, Waterman RS, Danka ES, Scandurro AB. Toll-like receptors on human mesenchymal stem cells drive their migration and immunomodulating responses. Stem Cells 2008;26:99–107.
33. Olson MA, Lee MS, Kissner TL, Alam S, Waugh DS, Saikh KU. Discovery of small molecule inhibitors of MyD88-dependent signaling pathways using a computational screen. Sci Rep 2015;5:14246.
34. O'Neill LAJ, Golenbock D, Bowie AG. The history of Toll-like receptors - redefining innate immunity. Nat Rev Immunol 2013;13:453–60.
35. Medema RH, Macurek L. Checkpoint control and cancer. Oncogene 2012; 31:2601–13.
36. Bode KA, Schroder K, Hume DA, Ravasi T, Heeg K, Sweet MJ, et al. Histone deacetylase inhibitors decrease Toll-like receptor-mediated activation of proinflammatory gene expression by impairing transcription factor recruitment. Immunology 2007;122:596–606.
37. Bode KA, Dalpke AH. HDAC inhibitors block innate immunity. Blood 2011;117:1102–3.
38. Roger T, Lugrin J, Le Roy D, Goy G, Mombelli M, Koessler T, et al. Histone deacetylase inhibitors impair innate immune responses to Toll-like receptor agonists and to infection. Blood 2011;117:1205–17.
39. Grabiec AM, Krausz S, de Jager W, Burakowski T, Groot D, Sanders ME, et al. Histone deacetylase inhibitors suppress inflammatory activation of rheumatoid arthritis patient synovial macrophages and tissue. J Immunol 2010;184:2718–28.
40. Sehn LH, Gascoyne RD. Diffuse large B-cell lymphoma: optimizing outcome in the context of clinical and biologic heterogeneity. Blood 2015;125:22–32.
41. Chng WJ, Schop RF, Price-Troska T, Ghobrial I, Kay N, Jelinek DF, et al. Gene-expression profiling of Waldenstrom macroglobulinemia reveals a phenotype more similar to chronic lymphocytic leukemia than multiple myeloma. Blood 2006;108:2755–63.
42. Liang BB, Chen R, Wang T, Cao L, Liu YY, Yin F, et al. Myeloid differentiation factor 88 promotes growth and metastasis of human hepatocellular carcinoma. Clin Cancer Res 2013;19:2905–16.